$K_L \to \pi^0 e^+ e^-$ and $B \to X_s l^+ l^-$ decay in the MSSM

Peter Cho

California Institute of Technology, Pasadena, California 91125

Mikołaj Misiak and Daniel Wyler

Institut für Theoretische Physik der Universität Zürich, Winterthurerstrasse 190, CH-8057 Zürich

The flavor changing neutral current processes $K_L \to \pi^0 e^+ e^-$, $B \to X_s e^+ e^-$, and $B \to X_s \mu^+ \mu^-$ are studied within the minimal supersymmetric extension of the standard model. We first examine the rates for these decay modes in the MSSM with a universal soft supersymmetry breaking sector at a grand unification scale. We later relax the universality condition and investigate the FCNC transitions in a more general class of models with negligible flavor violation in squark mixing matrices. We find that the MSSM prediction for the kaon channel's branching fraction differs from its standard model value by at most 30% over the entire allowed parameter space. On the other hand, supersymmetric contributions could potentially enhance certain $B \to X_s l^+ l^-$ observables by more than 100% relative to standard model expectations. The impact of supersymmetry upon the B meson modes is strongly correlated with the MSSM value for the Wilson coefficient of the magnetic moment operator that mediates $B \to X_s \gamma$. [S0556-2821(96)01917-0]

I. INTRODUCTION

The minimal supersymmetric standard model (MSSM) remains one of the few well-motivated extensions of the standard model which has survived precision electroweak measurements [1]. The need to subject this theory to other complementary experimental tests has consequently grown with time. Flavor changing neutral current (FCNC) phenomenology represents one area where data are stringently confronting the MSSM [2]. Deviations from the standard model may be observed in FCNC processes long before superpartners are detected at high-energy colliders. Alternatively, failure to detect such departures places constraints upon weak scale supersymmetry and all other theories of physics beyond the standard model. For example, the recent CLEO observation of inclusive $B \to X_s \gamma$ decay rules out charged Higgs bosons lighter than 260 GeV in two-Higgs-doublet models [3]. This lower bound lies far beyond the reach of present direct searches. The $B \to X_s \gamma$ measurement similarly constrains the MSSM, but its restrictive power is diminished by possible cancellations between different superparticle contributions [4]. It is therefore important to study the sensitivity of other FCNC processes to supersymmetry and determine their limiting capabilities.

In this work, we investigate the rare decays $K_L \to \pi^0 e^+ e^-$, $B \to X_s e^+ e^-$, and $B \to X_s \mu^+ \mu^-$ within the MSSM framework. Positive signals in these channels are expected to be observed within the next few years provided their rates do not lie significantly below standard model predictions. The current experimental upper bound on the first process $B(K_L \to \pi^0 e^+ e^-)_{\text{expt}} < 4.3 \times 10^{-9}$ [5] is 3 orders of magnitude larger than the anticipated standard model branching fraction. Yet this mode is expected to be detected at Fermilab following completion of the Main Injector [6]. Present CLEO and Collider Detector at Fermilab (CDF) exclusive limits on the second and third channels, $B(B^0 \to K^{*0} e^+ e^-)_{\text{CLEO}} < 1.6 \times 10^{-5}$ [7] and

$B(B^0 \to K^{*0} \mu^+ \mu^-)_{\text{CDF}} < 2.1 \times 10^{-5}$ [8], lie within an order of magnitude of standard model predictions. Evidence for short distance $b \to s l^+ l^-$ decay may therefore soon be seen with the upgraded CLEO detector and in the full run Ib Tevatron data set.

$K_L \to \pi^0 e^+ e^-$ and $B \to X_s l^+ l^-$ decay have both been extensively studied in the standard model. The impact of conventional QCD upon their rates can *a priori* be comparable to that from any new physics. Significant theoretical effort has therefore been directed during the past several years towards determining the precise size of strong interaction corrections to these weak transitions [9–12]. Progress has also been made in estimating the hadronic matrix elements that characterize the long-distance aspects of these processes. Chiral perturbation theory calculations indicate that the CP-conserving component of $K_L \to \pi^0 e^+ e^-$ decay is significantly smaller than the total CP-violating contribution, and the direct CP-violating portion is believed to dominate over its indirect counterpart[1] [13,14]. This kaon mode can thus provide an important window onto the nature of CP violation.

Much less is known about the rates at which the two semileptonic FCNC reactions proceed within the MSSM. The sensitivity of $K_L \to \pi^0 e^+ e^-$ to new supersymmetric physics has received little attention. We therefore examine the maximal variation in the MSSM rate for the kaon process relative to its standard model value in this work. Supersymmetric contributions to $B \to X_s l^+ l^-$ decay were previously considered by Bertolini *et al.* in [16]. These authors' conclusions need to be updated in light of the $B \to X_s \gamma$ measurement. The important constraint placed by the CLEO obser-

---

[1]This favorable hierarchy for CP-conserving and -violating contributions to $K_L \to \pi^0 e^+ e^-$ decay has recently been challenged in Ref. [15].

TABLE I. MSSM matter content.

Superfields	Fermions	Scalars
$Q_i = \begin{pmatrix} U_i \\ D_i \end{pmatrix}$	$q_i = \begin{pmatrix} u_i \\ d_i \end{pmatrix}$	$\tilde{q}_i = \begin{pmatrix} \tilde{u}_i \\ \tilde{d}_i \end{pmatrix}$
U_i^c	u_i^c	$\tilde{u}_i^c$
D_i^c	d_i^c	$\tilde{d}_i^c$
$L_i = \begin{pmatrix} N_i \\ E_i \end{pmatrix}$	$l_i = \begin{pmatrix} \nu_i \\ e_i \end{pmatrix}$	$\tilde{l}_i = \begin{pmatrix} \tilde{\nu}_i \\ \tilde{e}_i \end{pmatrix}$
E_i^c	e_i^c	$\tilde{e}_i^c$
$H_1 = \begin{pmatrix} H_1^0 \\ H_1^- \end{pmatrix}$	$\tilde{h}_1 = \begin{pmatrix} \tilde{h}_1^0 \\ \tilde{h}_1^- \end{pmatrix}$	$h_1 = \begin{pmatrix} h_1^{0*} \\ -h_1^- \end{pmatrix}$
$H_2 = \begin{pmatrix} H_2^+ \\ H_2^0 \end{pmatrix}$	$\tilde{h}_2 = \begin{pmatrix} \tilde{h}_2^+ \\ \tilde{h}_2^0 \end{pmatrix}$	$h_2 = \begin{pmatrix} h_2^+ \\ h_2^0 \end{pmatrix}$

vation upon the allowed MSSM parameter space was incorporated into the more recent $B \to X_s l^+ l^-$ analysis of [17], but the impact of a universal form for soft supersymmetry breaking terms was not studied in this latter work. As we shall see, inclusion of both the $B \to X_s \gamma$ restriction and the universality constraint disallows sizable deviations from the standard model in the integrated $B \to X_s l^+ l^-$ decay rate. Our work thus builds upon and extends previous supersymmetric FCNC investigations presented in the literature.

Our paper is organized as follows. In Sec. II, we review the elements of the MSSM which are relevant to our FCNC analysis. We then discuss current restrictions upon the MSSM parameter space in Sec. III and describe two different procedures for mapping out its allowed regions. We use these scanning algorithms to examine the impact of supersymmetry upon $K_L \to \pi^0 e^+ e^-$ and $B \to X_s l^+ l^-$ decay in Secs. IV and V. Finally, we close with a summary of our findings in Sec. VI.

II. THE MINIMAL SUPERSYMMETRIC STANDARD MODEL

The basic structure of the MSSM is well known and has been thoroughly discussed in the literature [18–20]. We therefore recall just those aspects of the theory which are pertinent to $K_L \to \pi^0 e^+ e^-$ and $B \to X_s l^+ l^-$ decay. We first display our nomenclature conventions for matter superfields and their left handed fermion and scalar components in Table I. The fields listed in the first five rows of this table carry a generation subscript which ranges over three family values. They are also assigned negative parities under a discrete Z_2 symmetry in order to forbid baryon- and lepton-number violating interactions. The Higgs fields appearing in the last two rows transform positively under this matter parity symmetry.

The chiral superfields in Table I enter into the superpotential

$$W = \mu H_1 H_2 + Y_{ij}^U Q_i U_j^c H_2 + Y_{ij}^D Q_i D_j^c H_1 + Y_{ij}^E L_i E_j^c H_1, \tag{2.1}$$

which governs the supersymmetry preserving interactions among matter fields.[2] After vector superfield terms are included, the supersymmetric Lagrangian schematically appears in component form as

$$\mathcal{L}_{\text{SUSY}} = -\frac{1}{4} F_G^{A\,\mu\nu} F_{G\,\mu\nu}^A + \overline{\lambda_G^A} i \slashed{D}_{AB} \lambda_G^B + (D^\mu \phi)^\dagger (D_\mu \phi) + \overline{\psi} i \slashed{D} \psi - \left[\left(\frac{dW}{d\Phi_i} \right)^* \left(\frac{dW}{d\Phi_i} \right) + \frac{1}{2} \left(\frac{\partial^2 W}{\partial \Phi_i \partial \Phi_j} \psi_i^T C \psi_j + \text{H.c.} \right) \right]_{\Phi \to \phi}$$

$$- \sqrt{2} g_G [\phi^\dagger T_G^A \lambda_G^{A\,T} C \psi + \text{H.c.}] - \frac{1}{2} g_G^2 (\phi^\dagger T_G^A \phi)(\phi^\dagger T_G^A \phi). \tag{2.2}$$

The index G labels the color, weak isospin and hypercharge factors in the standard model gauge group, and indices A and B range over the nonabelian subgroups' adjoint representations. All MSSM scalars are assembled into ϕ, while matter fermions and gauginos are respectively contained within the four-component left-handed ψ and λ fields.

Since supersymmetry is manifestly violated in the low energy world, the MSSM Lagrangian is supplemented with the soft supersymmetry breaking terms

$$\mathcal{L}_{\text{soft}} = -\frac{1}{2} [m_{\tilde{g}} \tilde{g}^{aT} C \tilde{g}^a + m_{\tilde{W}} \tilde{W}^{iT} C \tilde{W}^i + m_{\tilde{B}} \tilde{B}^T C \tilde{B} + \text{H.c.}] - m_1^2 h_1^\dagger h_1 - m_2^2 h_2^\dagger h_2 - \tilde{q}_i^\dagger (M_{\tilde{q}}^2)_{ij} \tilde{q}_j - \tilde{u}_i^{c\dagger} (M_{\tilde{u}^c}^2)_{ij} \tilde{u}_j^c - \tilde{d}_i^{c\dagger} (M_{\tilde{d}^c}^2)_{ij} \tilde{d}_j^c$$

$$- \tilde{l}_i^\dagger (M_{\tilde{l}}^2)_{ij} \tilde{l}_j - \tilde{e}_i^{c\dagger} (M_{\tilde{e}^c}^2)_{ij} \tilde{e}_j^c + [A_{ij}^U \tilde{q}_i \tilde{u}_j^c h_2 + A_{ij}^D \tilde{q}_i \tilde{d}_j^c h_1 + A_{ij}^E \tilde{l}_i \tilde{e}_j^c h_1 + B\mu h_1 h_2 + \text{H.c.}]. \tag{2.3}$$

---

[2] Our sign convention for contracting two SU(2) doublets is exemplified by the expansion $H_1 H_2 = H_1^0 H_2^0 - H_1^- H_2^+$ of the superpotential μ term.

In order to cut down the number of free parameters which enter into this expression to a manageable size, some relations among soft sector masses and couplings must be adopted. We shall first assume that the weak scale values of all the parameters in Eq. (2.3) are simply related to grand-unified theory (GUT) scale progenitors. The running gaugino masses $m_{\tilde{g}}(\mu)$, $m_{\tilde{w}}(\mu)$, and $m_{\tilde{B}}(\mu)$ then unify at $\mu = M_{\mathrm{GUT}}$ just like the gauge couplings. We also equate all scalar mass parameters with a single m_0 at the GUT scale. Finally, we set the trilinear interaction matrices $A^{U,D,E}$ equal to $A_0 Y^{U,D,E}$ at $\mu = M_{\mathrm{GUT}}$ where A_0 denotes a common proportionality constant.[3] Imposition of this universal structure upon soft supersymmetry breaking terms lends predictive power to the MSSM, but the assumed simplifications are quite strong. We will therefore later relax some of these constraints and investigate a more general class of supersymmetric models.

Renormalization group evolution of MSSM parameters down from the unification scale can generate a vacuum instability [21–23]. As the couplings in the scalar potential run, the neutral Higgs fields may at some point develop nonzero vacuum expectation values $\langle h_1^0 \rangle = v_1/\sqrt{2}$ and $\langle h_2^0 \rangle = v_2/\sqrt{2}$ which break electroweak symmetry. The numerical value $v = \sqrt{v_1^2 + v_2^2} = 246$ GeV for their mean is fixed by the W boson mass. But the ratio $\tan\beta = v_2/v_1$ remains a free parameter in the model. We restrict this ratio to the range $2 \leq \tan\beta \leq 55$ so that Landau poles do not develop in the top or bottom Yukawa couplings anywhere between the weak and GUT scales.

Electroweak symmetry breaking induces mixing among MSSM fields. In the matter sector, primed mass eigenstates are related to unprimed gauge eigenstate counterparts as follows:

$$u' = S^{U_L}u + S^{U_R}C\overline{u}^{cT}, \quad \tilde{u}\,' = \Gamma^U \begin{pmatrix} S^{U_L}\tilde{u} \\ S^{U_R}\tilde{u}^{c*} \end{pmatrix},$$

$$d' = S^{D_L}d - S^{D_R}C\overline{d}^{cT}, \quad \tilde{d}\,' = \Gamma^D \begin{pmatrix} S^{D_L}\tilde{d} \\ -S^{D_R}\tilde{d}^{c*} \end{pmatrix},$$

$$\nu' = S^{N_L}\nu, \quad \tilde{\nu}\,' = \Gamma^N S^{E_L}\tilde{\nu},$$

$$e' = S^{E_L}e - S^{E_R}C\overline{e}^{cT}, \quad \tilde{e}\,' = \Gamma^E \begin{pmatrix} S^{E_L}\tilde{e} \\ -S^{E_R}\tilde{e}^{c*} \end{pmatrix}. \quad (2.4)$$

The unitary S and Γ transformations rotate fermion and sfermion mass matrices into real and diagonal forms. The 3×3 quark and lepton mass matrices are simply related to the Yukawa couplings in the superpotential:

$$M_U = \frac{v\,\sin\beta}{\sqrt{2}} S^{U_R}Y^{UT}S^{U_L\dagger},$$

$$M_D = \frac{v\,\cos\beta}{\sqrt{2}} S^{D_R}Y^{DT}S^{D_L\dagger}, \quad (2.5)$$

$$M_E = \frac{v\,\cos\beta}{\sqrt{2}} S^{E_R}Y^{ET}S^{E_L\dagger}.$$

On the other hand, the 6×6 squared mass matrices for the squarks and sleptons look much more complicated and involve many parameters from both the supersymmetry conserving and violating Lagrangians in Eqs. (2.2) and (2.3):

$$M_{\tilde{u}}^2 = \Gamma^U \begin{pmatrix} S^{U_L}M_{\tilde{q}}^2 S^{U_L\dagger} + M_U^2 + \frac{m_Z^2}{6}(3 - 4\sin^2\theta)\cos 2\beta & \mu M_U \cot\beta - \frac{v\,\sin\beta}{\sqrt{2}} S^{U_L}A^{U*}S^{U_R\dagger} \\ \mu^* M_U \cot\beta - \frac{v\,\sin\beta}{\sqrt{2}} S^{U_R}A^{UT}S^{U_L\dagger} & S^{U_R}M_{\tilde{u}^c}^{2\,T}S^{U_R\dagger} + M_U^2 + \frac{2m_Z^2}{3}\sin^2\theta\,\cos 2\beta \end{pmatrix} \Gamma^{U\dagger},$$

$$M_{\tilde{d}}^2 = \Gamma^D \begin{pmatrix} S^{D_L}M_{\tilde{q}}^2 S^{D_L\dagger} + M_D^2 - \frac{m_Z^2}{6}(3 - 2\sin^2\theta)\cos 2\beta & \mu M_D \tan\beta - \frac{v\,\cos\beta}{\sqrt{2}} S^{D_L}A^{D*}S^{D_R\dagger} \\ \mu^* M_D \tan\beta - \frac{v\,\cos\beta}{\sqrt{2}} S^{D_R}A^{DT}S^{D_L\dagger} & S^{D_R}M_{\tilde{d}^c}^{2\,T}S^{D_R\dagger} + M_D^2 - \frac{m_Z^2}{3}\sin^2\theta\,\cos 2\beta \end{pmatrix} \Gamma^{D\dagger},$$

$$M_{\tilde{\nu}}^2 = \Gamma^N (S^{E_L}M_{\tilde{l}}^2 S^{E_L\dagger} + \tfrac{1}{2}m_Z^2\cos 2\beta)\Gamma^{N\dagger},$$

$$M_{\tilde{e}}^2 = \Gamma^E \begin{pmatrix} S^{E_L}M_{\tilde{l}}^2 S^{E_L\dagger} + M_E^2 - \frac{m_Z^2}{2}(1 - 2\sin^2\theta)\cos 2\beta & \mu M_E\tan\beta - \frac{v\,\cos\beta}{\sqrt{2}} S^{E_L}A^{E*}S^{E_R\dagger} \\ \mu^* M_E\tan\beta - \frac{v\,\cos\beta}{\sqrt{2}} S^{E_R}A^{ET}S^{E_L\dagger} & S^{E_R}M_{\tilde{e}^c}^{2\,T}S^{E_R\dagger} + M_E^2 - m_Z^2\sin^2\theta\,\cos 2\beta \end{pmatrix} \Gamma^{E\dagger}. \quad (2.6)$$

---

[3]We do not assume any *a priori* relationship between A_0 and B in Eq. (2.3).

Mixing also takes place in the gaugino and Higgs sectors. The physical Dirac chargino and Majorana neutralino eigenstates are linear combinations of left-handed W-inos, B-inos, and Higgsinos:

$$\widetilde{\chi}^- = U\begin{pmatrix} \widetilde{W}^- \\ \widetilde{h}_1^- \end{pmatrix} + V^* C\begin{pmatrix} \overline{\widetilde{W}^+}^T \\ \overline{\widetilde{h}_2^+}^T \end{pmatrix},$$

$$\widetilde{\chi}_M^0 = N\begin{pmatrix} \widetilde{B} \\ \widetilde{W}_3 \\ \widetilde{h}_1^0 \\ \widetilde{h}_2^0 \end{pmatrix} + N^* C\begin{pmatrix} \overline{\widetilde{B}}^T \\ \overline{\widetilde{W}_3}^T \\ \overline{\widetilde{h}_1^0}^T \\ \overline{\widetilde{h}_2^0}^T \end{pmatrix}. \tag{2.7}$$

The unitary transformations U, V, and N diagonalize these fields' mass matrices

$$M_{\widetilde{\chi}^\pm} = U^* \begin{pmatrix} m_{\widetilde{W}} & \sqrt{2}m_W \sin\beta \\ \sqrt{2}m_W \cos\beta & -\mu \end{pmatrix} V^\dagger \tag{2.8}$$

and

$$M_{\widetilde{\chi}^0} = N^* \begin{pmatrix} m_{\widetilde{B}} & 0 & -m_Z\sin\theta\,\cos\beta & m_Z\sin\theta\,\sin\beta \\ 0 & m_{\widetilde{W}} & m_Z\cos\theta\,\cos\beta & -m_Z\cos\theta\,\sin\beta \\ -m_Z\sin\theta\,\cos\beta & m_Z\cos\theta\,\cos\beta & 0 & \mu \\ m_Z\sin\theta\sin\beta & -m_Z\cos\theta\,\sin\beta & \mu & 0 \end{pmatrix} N^\dagger. \tag{2.9}$$

Similarly, charged scalar mass eigenstates are combinations of $h_1^\pm$ and $h_2^\pm$:

$$\begin{pmatrix} \pi^\pm \\ h^\pm \end{pmatrix} = \begin{pmatrix} \cos\beta & \sin\beta \\ -\sin\beta & \cos\beta \end{pmatrix} \begin{pmatrix} h_1^\pm \\ h_2^\pm \end{pmatrix}. \tag{2.10}$$

The $\pi^\pm$ would-be Goldstone bosons are absorbed via the Higgs mechanism into the longitudinal components of the $W^\pm$ gauge fields. But the remaining $h^\pm$ bosons represent genuine propagating scalar degrees of freedom whose tree level squared masses equal $m_{h^\pm}^2 = m_W^2 + m_1^2 + m_2^2 + 2|\mu|^2$.

After the gauge eigenstate fields in the supersymmetric Lagrangian (2.2) are rewritten in terms of their mass eigenstate counterparts,[4] it is straightforward to work out the interactions of gluinos, charginos and neutralinos with quarks and squarks. We list below the resulting terms which participate at one-loop order in $d_i \to d_j l^+ l^-$ decay:

$$\mathcal{L}_{\widetilde{g},\widetilde{\chi}} = -\sqrt{2}g_3 \sum_{a=1}^8 \overline{\widetilde{g}_M^a}\,\widetilde{d}^\dagger(\Gamma^{D_L}P_- - \Gamma^{D_R}P_+)T^a d$$
$$+ \sum_{I=1}^2 \overline{\widetilde{\chi}_I}\,\widetilde{u}^\dagger(X_I^{U_L}P_- + X_I^{U_R}P_+)d$$
$$+ \sum_{I=1}^4 (\overline{\widetilde{\chi}_M^0})_I\,\widetilde{d}^\dagger(Z_I^{D_L}P_- + Z_I^{D_R}P_+)d + \text{H.c.},$$

$$\tag{2.11}$$

where

---

[4] We suppress primes on mass eigenstates fields from here on.

$$X_I^{U_L} = g_2\left(-V_{I1}^*\Gamma^{U_L} + V_{I2}^*\Gamma^{U_R}\frac{M_U}{\sqrt{2}m_W\sin\beta}\right)K,$$

$$X_I^{U_R} = g_2\left(U_{I2}\Gamma^{U_L}K\frac{M_D}{\sqrt{2}m_W\cos\beta}\right),$$

$$\tag{2.12}$$

$$Z_I^{D_L} = -\frac{g_2}{\sqrt{2}}\left[\left(-N_{I2}^* + \frac{1}{3}\tan\theta N_{I1}^*\right)\Gamma^{D_L} + N_{I3}^*\Gamma^{D_R}\frac{M_D}{m_W\cos\beta}\right],$$

$$Z_I^{D_R} = -\frac{g_2}{\sqrt{2}}\left(\frac{2}{3}\tan\theta N_{I1}\Gamma^{D_R} + N_{I3}\Gamma^{D_L}\frac{M_D}{m_W\cos\beta}\right).$$

Flavor mixing enters into these interactions through the Kobayashi-Maskawa matrix $K = S^{U_L}S^{D_L\dagger}$ and the 6×3 block components of Γ^U and Γ^D:

$$\Gamma_{6\times6}^U = (\Gamma_{6\times3}^{U_L} \quad \Gamma_{6\times3}^{U_R}),$$

$$\Gamma_{6\times6}^D = (\Gamma_{6\times3}^{D_L} \quad \Gamma_{6\times3}^{D_R}). \tag{2.13}$$

Other gauge boson and Higgs terms which mediate the FCNC processes of interest are similarly extracted from the Lagrangian. The Feynman rules for all these interactions may be found in the literature [18,24].

Having set up the basic MSSM framework, we are now ready to explore its large parameter space. We take up this topic in the following section.

III. MSSM PARAMETER SPACE

Before predictions can be derived from the minimal supersymmetric standard model, explicit values for the parameters in the superpotential (2.1) and soft supersymmetry breaking Lagrangian (2.3) must be specified. In order to reduce the size of the parameter space, we initially adopt the common assumption that MSSM masses and couplings are simply related at $\mu = M_{\text{GUT}}$. This ansatz is motivated by the simplest supergravity theories [25]. A universal soft supersymmetry breaking sector at $\mu = M_{\text{GUT}}$ also decreases the likelihood of generating unacceptably large FCNC amplitudes at the weak scale. Instead, the magnitudes for such amplitudes in the MSSM are anticipated to be of the same order as those in the standard model. Experimentally discriminating between the two theories' predictions for various FCNC transitions rates will not be an easy task. But this goal is hoped to be achieved by a number of experimental programs within the next several years.

In our analysis, we take as input parameters the dimensionful soft sector quantities $A_0(M_{\text{GUT}})$, $m_0(M_{\text{GUT}})$, and $m_{\widetilde{W}}(m_z)$, the dimensionless ratio $\tan\beta$, and all standard model fermion and gauge boson masses and couplings. We also restrict the source of CP violation in the MSSM to stem from just a single phase in the KM matrix. Imaginary parts of $m_{\widetilde{W}}$ and $B\mu$ can be rotated away by field redefinitions, but A_0 and μ generally remain complex. The phases of these last two parameters are tightly constrained by neutron electric-dipole moment limits [26]. We shall simply take A_0 and μ to be real.

In order to determine the numerical values for all the couplings in the MSSM, we follow a lengthy yet straightforward procedure. We first locate the GUT scale $M_{\text{GUT}} \sim 10^{16}$ GeV by evolving the $SU(2)_L$ and $U(1)_Y$ gauge couplings up to the point where they meet. We then choose specific values for $A_0(M_{\text{GUT}})$, $m_0(M_{\text{GUT}})$, $m_{\widetilde{W}}(m_z)$, and $\tan\beta$. A large value for the trilinear scalar coupling in conjunction with small values for the common scalar and gaugino mass parameters tends to yield stop masses which are too light to satisfy direct search constraints. Large values for either m_0 or $m_{\widetilde{W}}$ lead to squark decoupling and negligible supersymmetric contributions to FCNC decays. We, therefore, restrict the magnitudes of the three dimensionful quantities to be less than 1 TeV.

After the gaugino, scalar, and Yukawa terms in the soft supersymmetry breaking sector are evaluated at $\mu = M_{\text{GUT}}$ and run down to $\mu = m_z$, the numerical values for all MSSM parameters except μ and B are determined. The tree-level relations

$$|\mu|^2 = \frac{m_2^2 \sin^2\beta - m_1^2 \cos^2\beta}{\cos 2\beta} - \frac{1}{2} m_Z^2,$$

$$B\mu = \frac{1}{2} \sin 2\beta (m_1^2 + m_2^2 + 2|\mu|^2), \qquad (3.1)$$

fix these last two quantities up to a twofold ambiguity in $\text{sgn}(\mu)$. Points in the MSSM parameter space which yield negative values for $|\mu|^2$ or $B\mu$ fail to break electroweak symmetry and are rejected. Necessary conditions for the existence of a stable scalar potential minimum

$$|B\mu|^2 > (m_1^2 + |\mu|^2)(m_2^2 + |\mu|^2),$$

$$(m_1^2 - m_2^2)\cos 2\beta > 0, \qquad (3.2)$$

must also be satisfied. The results appearing in Eqs. (3.1) and (3.2) originate from tree-level minimization of the classical scalar potential. Quantum corrections significantly shift the location of the effective potential minimum [28]. Radiative corrections can enhance light neutral Higgs boson masses by nearly a factor of 2 relative to tree-level predictions. But as we shall see, neutral Higgs contributions to $K_L \rightarrow \pi^0 e^+ e^-$ and $b \rightarrow s l^+ l^-$ decay are completely negligible. Moreover, changes in $|\mu|$ arising from loop corrections to Eq. (3.1) do not affect the qualitative conclusion that allowed values for $|\mu|$ are several times greater than m_z. We therefore utilize these tree-level relations in our numerical analysis.

Once numerical values for the MSSM parameters have been specified, the masses of all superpartners can be calculated. We require that the mass spectrum be consistent with present limits from direct superpartner searches [5]. In particular, we impose the recent LEP 1.5 lower bound of 65 GeV on the chargino mass [27].

The final constraint which we place upon the MSSM parameter space comes from $B \rightarrow X_s \gamma$ decay. Supersymmetry modifies the standard model prediction for the rare radiative rate by adding extra contributions to the Wilson coefficients $C_7(m_W)$ and $C_8(m_W)$ of the electromagnetic and chromomagnetic moment operators in the $\Delta B = 1$ effective Hamiltonian [29]. We neglect C_8 since it accounts for only 3% of the standard model $b \rightarrow s\gamma$ amplitude and is not expected to be significantly more important in the MSSM. But the charged Higgs, chargino, neutralino, and gluino contributions to C_7 which are tabulated in Appendix A can be quite substantial. We therefore calculate the ratio

$$R_7 = \frac{C_7(m_W)_{\text{MSSM}}}{C_7(m_W)_{\text{SM}}} \qquad (3.3)$$

at each point in the MSSM parameter space. We throw away all points whose values for R_7 do not lie within the allowed intervals

$$0.4 < R_7 < 1.2 \quad \text{or} \quad -4.2 < R_7 < -2.4 \qquad (3.4)$$

that take into account current experimental errors [3] and theoretical uncertainties [29].

After scanning over the MSSM parameter space and imposing all the above criteria, we identify a number of general features which hold everywhere in the allowed regions except in the very large $\tan\beta$ domain:

(i) Sizable supersymmetry contributions to $K_L \rightarrow \pi^0 e^+ e^-$, $B \rightarrow X_s l^+ l^-$, and $B \rightarrow X_s \gamma$ decay mainly arise from charged Higgs and chargino exchange.

(ii) Flavor violating entries in Γ^u hardly affect these FCNC processes.

(iii) The first two generations of up and down squarks are almost degenerate. The first two generations of sleptons and sneutrinos are also nearly degenerate.

(iv) Left-right squark and slepton mixing is negligible for the first two generations.

Similar observations have previously been noted in [16].

These characteristics provide useful guidelines for establishing less restrictive constraints on supersymmetric extensions of the standard model than those which underlie the MSSM with a universal soft breaking sector. Rather than starting with a unified set of GUT scale parameters and evolving them down to low energies, we can instead survey all possible values for MSSM couplings and masses at the weak scale for which conditions (i)–(iv) are satisfied. This alternate mapping procedure provides a useful check on the sensitivity of FCNC results upon the assumed form of the soft supersymmetry breaking sector. The particular weak scale quantities which must be specified in order to determine supersymmetric contributions to $d_i \to d_j l^+ l^-$ decay are the following: a common mass $m_{\bar{u}_L}$ for the superpartners of left-handed up and charm quarks; the masses $m_{\bar{t}_L}$, $m_{\bar{t}_R}$ and mixing angle $\alpha_{\bar{t}}$ for top squarks; a common mass $m_{\bar{\nu}}$ for the first two generation sneutrinos; the Wino and charged Higgs masses $m_{\tilde{W}}$ and $m_{h^\pm}$; the superpotential μ parameter and $\tan\beta$. This parametrization is similar in spirit to the one adopted in [17]. As in our universal soft sector analysis, we shall restrict the dimensionful quantities to the sub-TeV regime and restrict the dimensionless VEV ratio to $2 \leq \tan\beta \leq 55$.

In the next two sections, we will investigate the $K_L \to \pi^0 e^+ e^-$ and $B \to X_s l^+ l^-$ transitions utilizing the universal soft sector scanning procedure as well as the more general mapping method. The greater labor required to explore the much larger nine-dimensional parameter space in the latter approach is offset by several simplifications. For example, neutralino and gluino contributions to $d_i \to d_j l^+ l^-$ may simply be neglected. The Γ_u matrix also reduces to the nearly diagonal form

$$\Gamma^U = \begin{pmatrix} 1 & 0 & 0 & 0 & 0 & 0 \\ 0 & 1 & 0 & 0 & 0 & 0 \\ 0 & 0 & \cos\alpha_{\bar{t}} & 0 & 0 & -\sin\alpha_{\bar{t}} \\ 0 & 0 & 0 & 1 & 0 & 0 \\ 0 & 0 & 0 & 0 & 1 & 0 \\ 0 & 0 & \sin\alpha_{\bar{t}} & 0 & 0 & \cos\alpha_{\bar{t}} \end{pmatrix} \quad (3.5)$$

when criteria (i)–(iv) are imposed. But most importantly, no renormalization group evolution needs to be performed. Searching the nine-dimensional parameter space for sets of points where supersymmetry significantly enhances or suppresses the rare decay modes is thus rendered tractable.

IV. $K_L \to \pi^0 e^+ e^-$ DECAY

The total amplitude for $K_L \to \pi^0 e^+ e^-$ decay can be decomposed into CP-conserving and violating parts. The former starts at second order in the electromagnetic interaction. As a result, the CP-conserving branching fraction $B(K_L \to \pi^0 e^+ e^-)_{CP} \simeq (0.3–1.8) \times 10^{-12}$ is significantly smaller than its CP-violating counterpart [13]. Moreover, the indirect component of the CP-violating amplitude is believed to be smaller than the direct part. Present data imply $B(K_L \to \pi^0 e^+ e^-)_{\text{indirect}} \leq 1.6 \times 10^{-12}$ [14], while the standard model prediction for the direct CP-violating contribution lies in the range $B(K_L \to \pi^0 e^+ e^-)_{\text{direct}}$

$\simeq (2.5–9.0) \times 10^{-12}$ [11].[5] The CP-conserving and indirect CP-violating amplitudes may be computed using experimentally determined values for chiral Lagrangian coefficients and the ϵ parameter which automatically include possible MSSM contributions. Since these quantities are consistent with standard model predictions, we will focus exclusively upon the direct CP-violating component in our supersymmetric FCNC investigation.

The analysis of $K_L \to \pi^0 e^+ e^-$ decay is greatly facilitated by working within an effective field theory framework. In this approach, heavy degrees of freedom are successively integrated out from a specified full theory, and the resulting effective theory is run down to a low energy hadronic scale using the renormalization group. A finite number of flavor changing dimension-six operators generated by this process at $\mu = m_W$ enter into the effective Hamiltonian $\mathcal{H}_{\text{eff}}$ which governs the dynamics of the low energy theory. The complete set of left-handed $\Delta S = 1$ four-fermion operators that originate from the standard model and mediate $K_L \to \pi^0 e^+ e^-$ are catalogued in Ref. [11]. If the starting full theory is taken to be the MSSM, additional terms with right-handed flavor changing currents appear in $\mathcal{H}_{\text{eff}}$. But since their coefficients are tiny, the extra operators may be neglected without loss.

After the effective theory is evolved to low energies, the direct CP-violating $K_L \to \pi^0 e^+ e^-$ amplitude is well approximated by the long-distance matrix element $\langle \pi^0 e^+ e^- | \mathcal{H}_{\text{eff}} | K_L \rangle$ of the truncated Hamiltonian

$$\mathcal{H}_{\text{eff}} = -\frac{G_F}{\sqrt{2}} K_{ts}^* K_{td} [y_{7V} Q_{7V} + y_{7A} Q_{7A}] + \text{H.c.} \quad (4.1)$$

All information associated with short distance physics is encoded into the Wilson coefficients

$$y_{7V} = \frac{\alpha_{\text{EM}}}{2\pi \sin^2\theta} \left[P_0 + [Y(x_t) + Y^{\text{SUSY}}] \right.$$
$$\left. -4\sin^2\theta (Z(x_t) + Z^{\text{SUSY}}) + P_E(E(x_t) + E^{\text{SUSY}}) \right],$$

$$y_{7A} = -\frac{\alpha_{\text{EM}}}{2\pi \sin^2\theta} [Y(x_t) + Y^{\text{SUSY}}], \quad (4.2)$$

of the semileptonic operators

$$Q_{7V} = \bar{s}\gamma^\mu(1-\gamma^5)d\,\bar{e}\gamma_\mu e,$$

$$Q_{7A} = \bar{s}\gamma^\mu(1-\gamma^5)d\,\bar{e}\gamma_\mu\gamma^5 e. \quad (4.3)$$

The functions

$$Y(x_t) = \frac{4x_t - x_t^2}{8(1-x_t)} + \frac{3x_t^2}{8(1-x_t)^2} \ln x_t$$

---

[5]The sizable uncertainty in the direct CP-violating branching fraction primarily stems from KM angles which are poorly constrained at present. The predictions' precision should substantially improve when the KM unitarity triangle is better determined in upcoming B-factory studies.

$$Z(x_t) = \frac{108x_t - 259x_t^2 + 163x_t^3 - 18x_t^4}{144(1-x_t)^3}$$

$$+ \frac{-8 + 50x_t - 63x_t^2 - 6x_t^3 + 24x_t^4}{72(1-x_t)^4} \ln x_t,$$

$$E(x_t) = \frac{18x_t - 11x_t^2 - x_t^3}{12(1-x_t)^3} - \frac{4 - 16x_t + 9x_t^2}{6(1-x_t)^4} \ln x_t \quad (4.4)$$

of the variable $x_t = (m_t/m_W)^2$ summarize the high energy contributions to $K_L \to \pi^0 e^+ e^-$ decay that are common to both the standard model and MSSM. Next-to-leading order QCD corrections which are the same in both theories are incorporated into $P_0 \simeq 0.7$ and $P_E \simeq -0.01$ [11]. Therefore, all effects of supersymmetry upon the rare weak transition reside within the Y^{SUSY}, Z^{SUSY}, and E^{SUSY} parameters in Eq. (4.2).

The values of the y_{7V} and y_{7A} coefficients are obtained after matching renormalized $\bar{s} \to \bar{d} e^+ e^-$ amplitudes calculated in both the full and effective theories. We perform this matching at $\mu = m_W$ in the standard model as well as in its minimal supersymmetric extension. The one-loop bubble, penguin, and box graphs which must be evaluated on the MSSM side of the matching condition are displayed in Figs. 1(a)–1(c). After a long but straightforward computation, we find the charged Higgs, chargino, neutralino, and gluino con-

tributions listed in Appendix B to the Y^{SUSY} and Z^{SUSY} terms in Eq. (4.2).

Several points about our supersymmetric matching results should be noted. Firstly, we have not included any bubble or penguin graphs which involve neutral Higgs boson exchange in Figs. 1(a) or 1(b). Such diagrams are proportional to the electron mass m_e and are negligibly small. Similarly, the first box graph in Fig. 1(c) with a charged Higgs running around the loop vanishes in the $m_e \to 0$ limit and may be safely ignored. Secondly, we have intentionally not calculated E^{SUSY} which should be comparable in size to $E(x_t) \simeq 0.25$. Since the numerical value for P_E is almost two orders of magnitude smaller than that for P_0, the term proportional to P_E in Eq. (4.2) is negligible and E^{SUSY} is unimportant. Thirdly, we have ignored gluino loop matching contributions to charged current four-quark operators in the $\Delta S = 1$ effective Hamiltonian. Such contributions affect y_{7V} and y_{7A} at the subpercent level. Finally, the matching condition results displayed in Appendix B are independent of any choice for the structure of soft supersymmetry breaking terms.

The short distance y_{7V} and y_{7A} Wilson coefficients enter into the direct CP-violating $K_L \to \pi^0 e^+ e^-$ partial width along with a long distance hadronic matrix element. After neglecting tiny imaginary components in the former quantities and relating the latter to the measured $K^+ \to \pi^0 e^+ \nu$ rate via an isospin rotation, we find [11]

$$B(K_L \to \pi^0 e^+ e^-)_{\text{direct}} = B(K^+ \to \pi^0 e^+ \nu) \frac{\tau(K_L)}{\tau(K^+)} \left| \frac{\text{Im}(K_{ts}^* K_{td})}{K_{us}} \right|^2 (y_{7V}^2 + y_{7A}^2). \quad (4.5)$$

The sensitive dependence of this expression upon poorly known KM angles can be removed by normalizing the MSSM branching fraction to its standard model analogue. The ratio

$$\rho(K_L \to \pi^0 e^+ e^-) = \frac{B(K_L \to \pi^0 e^+ e^-)_{\text{MSSM}} - B(K_L \to \pi^0 e^+ e^-)_{\text{SM}}}{B(K_L \to \pi^0 e^+ e^-)_{\text{SM}}} \quad (4.6)$$

thus cleanly quantifies supersymmetric enhancement or suppression of the rare kaon mode's rate.

Following the universal soft sector scanning procedure outlined in Sec. III, we evaluate $\rho(K_L \to \pi^0 e^+ e^-)$ in the allowed regions of MSSM parameter space. Representative results for two-dimensional slices through this space are illustrated in Figs. 2(a) and 2(b). In the first Lego block figure, $\rho(K_L \to \pi^0 e^+ e^-)$ is plotted as a function of $A_0(M_{\text{GUT}})$ and $m_0(M_{\text{GUT}})$ with $m_{\tilde{W}}(m_z) = 90$ GeV and $\tan \beta = 5.0$ held fixed. In the second figure, we display $\rho(K_L \to \pi^0 e^+ e^-)$ as a function of $m_{\tilde{W}}(m_z)$ and $\tan \beta$ with $A_0(M_{\text{GUT}}) = -500$ GeV and $m_0(M_{\text{GUT}}) = 100$ GeV. We have taken the sign of the μ parameter in the superpotential to be positive in both plots. Points in the MSSM parameter space that are excluded by one or more of our imposed criteria are indicated in these figures by Lego blocks which are saturated at their maximum values. Looking at the results in Figs. 2(a) and 2(b), we see that supersymmetric effects in the MSSM with a universal soft sector reduce the direct CP-violating $K_L \to \pi^0 e^+ e^-$ branching fraction relative to the expected standard model

rate by at most 10%. These discrepancies between the standard model and its minimal supersymmetric extension are unfortunately too small to be realistically detected by upcoming experiments within the next several years.

It is interesting to examine whether larger deviations could result if some of the stringent assumptions underlying the universal soft sector MSSM are relaxed. We have therefore performed several scans involving hundreds of thousands of points over the more general nine-dimensional parameter space discussed in Sec. III. These scans reveal that pockets in the larger space exist where discrepancies between the standard model and the MSSM are three times larger in both the positive and negative directions than those we previously uncovered in our more restricted searches. But even a 30% supersymmetric enhancement or suppression of the $K_L \to \pi^0 e^+ e^-$ rate relative to its standard model value is unlikely to be experimentally resolvable in the near future.

The potential impact of supersymmetry upon the rare kaon mode is thus disappointingly small. But as we shall see in the next section, the prospects for detecting signs of supersymmetry in $B \to X_s l^+ l^-$ decay are brighter.

FIG. 1. One-loop MSSM (a) bubble, (b) penguin, and (c) box graphs which contribute to the short distance coefficients of effective theory operators that mediate $K_L \to \pi^0 e^+ e^-$ and $B \to X_s l^+ l^-$ decay.

V. $B \to X_s e^+ e^-$ AND $B \to X_s \mu^+ \mu^-$ DECAY

Inclusive $B \to X_s e^+ e^-$ and $B \to X_s \mu^+ \mu^-$ decay share several similarities with the $K_L \to \pi^0 e^+ e^-$ transition. Like their kaon analogue, these B meson reactions are most conveniently analyzed within a low energy effective theory framework. The complete list of dimension-six operators in the $\Delta B = 1$ effective Hamiltonian that participate in $B \to X_s l^+ l^-$ decay may be found in Ref. [30]. The Wilson coefficients of the bottom sector operators evaluated at the W scale are trivially related to their strange sector analogues. The next-to-leading order evolution of these coefficients from $\mu = m_W$ to $\mu = m_b$ has been calculated in Ref. [12]. The details of this strong interaction running are quite complicated, and we will not present them here. Instead, we will simply apply the main results in our study of supersymmetric effects upon the rare decay modes.

The inclusive rate for the meson level process $B \to X_s l^+ l^-$ may be approximated by the rate for the free quark transition $b \to s l^+ l^-$ [31]. Two independent variables are required to describe the latter process. We choose them to be the rescaled lepton energies

$$y_+ = \frac{2E_{l^+}}{m_b} \quad \text{and} \quad y_- = \frac{2E_{l^-}}{m_b} \tag{5.1}$$

measured in the b quark rest frame. When expressed in terms of these variables along with the rescaled squared invariant mass $\hat{s} = y_+ + y_- - 1$ of the lepton pair, the differential decay rate looks like

$$\frac{d^2\Gamma(b \to s l^+ l^-)}{dy_+ dy_-} = \frac{G_F^2 m_b^5 |K_{ts}^* K_{tb}|^2}{16\pi^3} \left(\frac{\alpha_{\text{EM}}}{4\pi}\right)^2 \left\{ [y_+(1-y_+) + y_-(1-y_-)][|C_g^{\text{eff}}(\hat{s})|^2 + C_{10}^2] + \frac{4}{\hat{s}}\left(\hat{s}(1-\hat{s}) + (1-y_+)^2 \right.\right.$$
$$\left.\left. + (1-y_-)^2 + \frac{2m_l^2}{\hat{s}m_b^2}\right)(C_7^{\text{eff}})^2 + 4(1-\hat{s})C_7^{\text{eff}} \,\text{Re}[C_9^{\text{eff}}(\hat{s})] + 2(y_+ - y_-)C_{10}[2C_7^{\text{eff}} + \hat{s} \,\text{Re}[C_9^{\text{eff}}(\hat{s})]] \right\}. \tag{5.2}$$

The quantities

$$C_7^{\text{eff}} = C_7(m_w)\eta^{16/23} + \frac{8}{3} C_8(m_w)(\eta^{14/23} - \eta^{16/23}) + \sum_{i=1}^{8} h_i \eta^{a_i}, \tag{5.3a}$$

$$C_9^{\text{eff}} = \left(\frac{\pi}{\alpha_s(m_w)} + \frac{\omega(\hat{s})}{\eta}\right)\left(-0.1875 + \sum_{i=1}^{8} p_i \eta^{a_i+1}\right) + \frac{Y(x_t) + Y^{\text{SUSY}}}{\sin^2\theta} - 4[Z(x_t) + Z^{\text{SUSY}}] + [E(x_t) + E^{\text{SUSY}}]$$
$$\times \left(0.1405 + \sum_{i=1}^{8} q_i \eta^{a_i+1}\right) + 1.2468 + \sum_{i=1}^{8} \eta^{a_i}\left[r_i + s_i\eta + t_i h\left(\frac{m_c}{m_b}, \hat{s}\right) + u_i h(1, \hat{s}) + v_i h(0, \hat{s})\right], \tag{5.3b}$$

$$C_{10} = -\frac{Y(x_t) + Y^{\text{SUSY}}}{\sin^2\theta} \tag{5.3c}$$

that enter into the partial width depend upon the strong interaction coupling ratio $\eta = \alpha_s(m_w)/\alpha_s(m_b)$ and various matching condition functions which we previously encountered in our $K_L \to \pi^0 e^+ e^-$ analysis. The effective coefficients also involve the components of the following eight-dimensional vectors:

$$a_i = (0.6087, 0.6957, 0.2609, -0.5217, 0.4086, -0.4230, -0.8994, 0.1456),$$

$$h_i = (2.2996, -1.0880, -0.4286, -0.0714, -0.6494, -0.0380, -0.0186, -0.0057),$$

$$p_i = (0, 0, -0.3941, 0.2424, 0.0433, 0.1384, 0.1648, -0.0073),$$

$$q_i = (0, 0, 0, 0, 0.0318, 0.0918, -0.2700, 0.0059),$$

$$r_i = (0, 0, 0.8331, -0.1219, -0.1642, 0.0793, -0.0451, -0.1638), \tag{5.4}$$

$$s_i = (0, 0, -0.2009, -0.3579, 0.0490, -0.3616, -0.3554, 0.0072),$$

$$t_i = (0, 0, 1.7143, -0.6667, 0.1658, -0.2407, -0.0717, 0.0990),$$

$$u_i = (0, 0, 0, 0.2857, 0, -0.2559, 0.0083, 0.0180, -0.0562),$$

$$v_i = (0, 0, 0.1429, 0.1667, -0.1731, -0.1120, -0.0178, -0.0067).$$

Finally, the functions $h(z,\hat{s})$ and $\omega(\hat{s})$ which appear in Eq. (5.3b) are given by

$$h(z,\hat{s}) = -\frac{8}{9}\ln z + \frac{8}{27} + \frac{4}{9}x - \frac{2}{9}(2+x)\sqrt{|1-x|}\begin{cases} \ln\left|\dfrac{\sqrt{1-x}+1}{\sqrt{1-x}-1}\right| - i\pi & \text{for } x \equiv 4z^2/\hat{s} < 1, \\[2mm] 2\arctan(1/\sqrt{x-1}) & \text{for } x \equiv 4z^2/\hat{s} > 1, \end{cases}$$

$$\omega(\hat{s}) = -\frac{4}{3}\text{Li}_2(\hat{s}) - \frac{2}{3}\ln(\hat{s})\ln(1-\hat{s}) - \frac{2}{9}\pi^2 - \frac{5+4\hat{s}}{3(1+2\hat{s})}\ln(1-\hat{s}) - \frac{2\hat{s}(1+\hat{s})(1-2\hat{s})}{3(1-\hat{s})^2(1+2\hat{s})}\ln(\hat{s}) + \frac{5+9\hat{s}-6\hat{s}^2}{6(1-\hat{s})(1+2\hat{s})}.$$

$$(5.5)$$

In order to consistently compute the differential rate to one-loop order accuracy, we only retain terms in $d^2\Gamma/dy_+dy_-$ up to linear order in $\omega(\hat{s})$. We also set $\omega(\hat{s})$ to zero in the interference terms in Eq. (5.2) which are proportional to $\text{Re}[C_9^{\text{eff}}(\hat{s})]$.

The standard model prediction for the $B\to X_s l^+l^-$ decay rate is simply recovered from these formulas by setting Y^{SUSY}, Z^{SUSY}, and E^{SUSY} to zero and equating $C_7(m_w)$ and $C_8(m_w)$ with their standard model values. In this case, the partially integrated rate $d\Gamma/d\hat{s}$ differs from the corresponding result discussed in [12] by a term proportional to the lepton mass. This term was previously neglected because its effect is very small over nearly all of phase space. However, its contribution to the integrated decay rate is not suppressed by m_l provided no lower cut on $\hat{s}$ is imposed. As no such cut has been performed in the recent CDF analysis of $B\to K^*\mu^+\mu^-$ [8], we retain this additional term in $d\Gamma/d\hat{s}$.

The matching condition expressions for Y^{SUSY} and Z^{SUSY} that enter into the differential rate for $B\to X_s e^+e^-$ trivially differ from those for $K_L\to\pi^0e^+e^-$ by just the flavor label renamings specified in Appendix B. As in our previous $K_L\to\pi^0e^+e^-$ matching computation, we neglect E^{SUSY} and set $C_8(m_w)$ to zero. For the $B\to X_s\mu^+\mu^-$ mode, slepton and sneutrino indices must also be transformed from the first to second generation. The numerical values for individual matching contributions to Y^{SUSY} and Z^{SUSY} turn out to be almost identical for all three FCNC channels which we consider in this paper. The flavor independence of Y^{SUSY} and Z^{SUSY} implies that regions of the $B\to X_s l^+l^-$ spectrum dominated by C_9^{eff} and C_{10} are no more sensitive to supersymmetry than $K_L\to\pi^0e^+e^-$ decay. Sizable discrepancies between the standard model and its minimal supersymmetric extension can therefore only arise in $B\to X_s l^+l^-$ observables which depend to a large extent upon C_7^{eff}.

We should note an interesting point regarding the supersymmetric limit of these matching results. The approximate cancellation between different superpartner contributions to $B\to X_s\gamma$ decay has been interpreted as a manifestation of $\Gamma(b\to s\gamma)=0$ in the supersymmetric limit [4]. Since the magnetic moment operator which mediates the radiative transition belongs to a linear multiplet, it cannot arise in a fully supersymmetric effective Hamiltonian [32]. No analogous argument can be made for $b\to sl^+l^-$ decay. Penguin and box diagrams generate effective four-fermion operators that form the highest components of vector superfields. Such D terms survive in the limit of exact supersymmetry.

As low statistics will most likely hinder experimental determination of the full differential spectrum, we need to consider various integrated observables. Following the CDF analysis presented in [8], we first integrate the rate over the lepton pair mass regions

$$m_{l^+l^-} \in (2m_l, 2.9 \text{ GeV}) \cup (3.3 \text{ GeV}, 3.6 \text{ GeV}) \cup (3.8 \text{ GeV}, 4.6 \text{ GeV}). \quad (5.6)$$

These disjoint intervals exclude $m_{l^+l^-}$ values for which the inclusive $B\to X_s l^+l^-$ rate is dominated by intermediate J/ψ and ψ' states. By restricting our analysis to just this nonresonant region, we ensure the validity of the free quark approximation to inclusive B meson decay.

It is customary to reduce the uncertainties in the $b\to sl^+l^-$ partial width by normalizing it to the semileptonic rate

$$\Gamma(b\to ce^+\nu) = \frac{G_F^2 m_b^5 |K_{cb}|^2}{192\pi^3} g\left(\frac{m_c}{m_b}\right)\left\{1 - \frac{2\alpha_s(m_b)}{3\pi}\left[\left(\pi^2 - \frac{31}{4}\right)\left(1-\frac{m_c}{m_b}\right)^2 + \frac{3}{2}\right]\right\} \quad (5.7)$$

which is related to the measured branching ratio $B(B\to X_c e^+\nu)=0.104\pm0.004$ [5]. The function

$$g(z) = 1 - 8z^2 + 8z^6 - z^8 - 24z^4\ln z \quad (5.8)$$

appearing in this rate formula represents a phase space suppression factor. The sensitive dependence of $\Gamma(b\to sl^+l^-)$ and $\Gamma(b\to ce^+\nu)$ upon KM angles cancels in their ratio. However, errors in the numerical evaluation of the $B\to X_s l^+l^-$ partial width can be reduced to only the 10–20 % range due to uncertainties in quark masses and interference effects from excited charmonium states [33]. Therefore, signals of new physics beyond the standard model will be detectable only if they significantly exceed this level.

After integrating the differential rate in Eq. (5.2), expressing the result in terms of the ratios

$$R_7 = \frac{C_7(m_w)_{\mathrm{MSSM}}}{C_7(m_w)_{\mathrm{SM}}}, \quad R_Y = \frac{Y(x_t) + Y^{\mathrm{SUSY}}}{Y(x_t)},$$

and

$$R_Z = \frac{Z(x_t) + Z^{\mathrm{SUSY}}}{Z(x_t)}, \tag{5.9}$$

and adopting the parameter values $m_c = 1.3$ GeV, $m_b = 4.7$ GeV, $m_t = 176$ GeV, $\alpha_s(m_z) = 0.118$, and $|K_{ts}^* K_{tb}/K_{cb}|^2$ $|K_{ts}^* K_{tb}/K_{cb}|^2 = 0.95$, we find the following nonresonant branching fractions:

$$B(B \rightarrow X_s e^+ e^-)_{\mathrm{NR}} = 3.0 \times 10^{-7}[5.5 + 2.3 R_7^2 + 17.6 R_Y^2$$
$$+ 3.7 R_Z^2 - 2.1 R_7 R_Y + 1.4 R_7 R_Z - 11.5 R_Y R_Z + 4.6 R_7$$
$$+ 8.1 R_Y - 5.3 R_Z], \tag{5.10}$$

$$B(B \rightarrow X_s \mu^+ \mu^-)_{\mathrm{NR}} = 3.0 \times 10^{-7}[2.9 + 0.8 R_7^2 + 17.5 R_Y^2$$
$$+ 3.7 R_Z^2 - 2.1 R_7 R_Y + 1.4 R_7 R_Z - 11.4 R_Y R_Z + 0.7 R_7$$
$$+ 8.1 R_Y - 5.3 R_Z]. \tag{5.11}$$

The standard model values 7.3×10^{-6} and 4.9×10^{-6} for the $B \rightarrow X_s e^+ e^-$ and $B \rightarrow X_s \mu^+ \mu^-$ branching ratios are recovered by setting $R_7 = R_Y = R_Z = 1$ in these formulas.

The second $b \rightarrow s l^+ l^-$ observable we consider is the lepton-antilepton energy asymmetry

$$\mathcal{A} = \frac{N(E_{l^-} > E_{l^+}) - N(E_{l^+} > E_{l^-})}{N(E_{l^-} > E_{l^+}) + N(E_{l^+} > E_{l^-})}. \tag{5.12}$$

Here $N(E_{l^-} > E_{l^+})$ denotes the number of lepton pairs whose negatively charged member is more energetic in the B meson rest frame than its positive partner. Since $\mathcal{A}$ is odd under charge conjugation whereas $B(B \rightarrow X_s l^+ l^-)$ is even, the information about the differential spectrum encoded into the former observable does not overlap with that contained within the latter. The value for $\mathcal{A}$ is most simply determined for charged $B^\pm$ mesons which do not suffer from complications associated with $B - \bar{B}$ mixing. Counting only those lepton pairs whose invariant mass lies within the intervals specified in Eq. (5.6), we find

$$\mathcal{A}_{\mathrm{NR}} = \frac{3.0 \times 10^{-7}}{B(B \rightarrow X_s l^+ l^-)_{\mathrm{NR}}}[1.2 - 1.0 R_7 + 4.0 R_Y - 2.6 R_Z] R_Y. \tag{5.13}$$

This expression yields 7 and 10 % for $B \rightarrow X_s e^+ e^-$ and $B \rightarrow X_s \mu^+ \mu^-$ in the standard model, respectively.

Since deviations of R_Y and R_Z from unity over the allowed MSSM parameter space are small, supersymmetric effects in the $B \rightarrow X_s l^+ l^-$ channel critically depend upon the ratio R_7. In order to isolate the FCNC mode's sensitivity to this quantity, it is instructive to first artificially set $R_7 = 1$ everywhere throughout the region of MSSM parameter space allowed by all constraints. We then find that supersymmetric effects upon $B \rightarrow X_s l^+ l^-$ are quite similar to those for

$K_L \rightarrow \pi^0 e^+ e^-$. Nonresonant $B \rightarrow X_s l^+ l^-$ branching ratios are suppressed by at most 10% relative to their standard model values when GUT-scale universality is imposed, and changes in lepton asymmetries are even smaller. If the universal soft sector assumptions are relaxed, B meson rates and asymmetries then deviate from standard model predictions by at most 30%.

Of course, the value for the Wilson coefficient of the magnetic moment operator does not coincide in most regions of MSSM parameter space with its standard model counterpart. When GUT-scale universality is assumed and all but $B \rightarrow X_s \gamma$ constraints are imposed, we find that R_7 smoothly varies between -2.5 and 3 for large values of $\tan \beta$ and
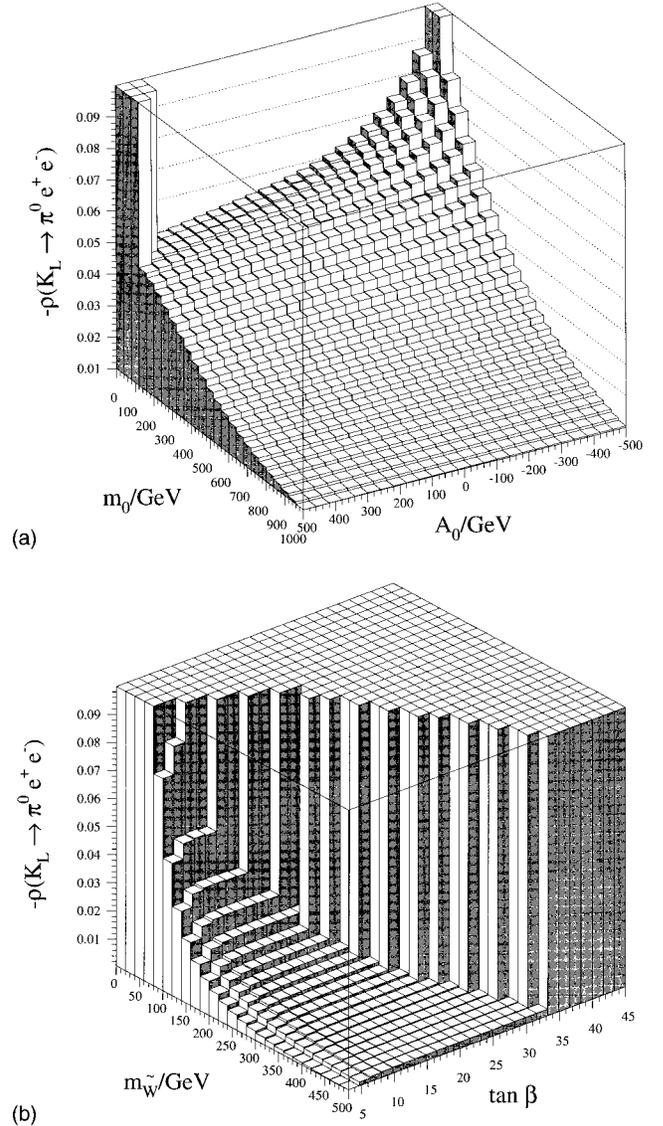

FIG. 2. Fractional suppression $\rho(K_L \rightarrow \pi^0 e^+ e^-)$ of the direct CP-violating component of the $K_L \rightarrow \pi^0 e^+ e^-$ branching fraction in the MSSM relative to the standard model prediction. The suppression factor is plotted in (a) as a function of $A_0(M_{\mathrm{GUT}})$ and $m_0(M_{\mathrm{GUT}})$ with $m_{\widetilde{W}}(m_z) = 90$ GeV and $\tan \beta = 5$ held fixed. The same quantity is displayed in (b) as a function of $m_{\widetilde{W}}(m_z)$ and $\tan \beta$ with $A_0(M_{\mathrm{GUT}}) = -500$ GeV and $m_0(M_{\mathrm{GUT}}) = 100$ GeV. Excluded MSSM parameter space points are indicated in both plots by Lego blocks saturated at their maximum values.

between 1.0 and 1.3 for $\tan\beta \approx 2.5$. This $\tan\beta$ dependence primarily stems from the $1/\cos\beta = \sqrt{1 + \tan^2\beta}$ enhancement of the chargino interaction matrix $X_I^{U_R}$ in Eq. (2.12). If we instead search over the nine-dimensional parameter space discussed in Sec. III, we find that R_7 ranges at the factor of 2 level from $-\tan\beta$ to $\tan\beta$. This potentially large R_7 variation underscores the stringent nature of the limits in Eq. (3.4) set by the CLEO $B \to X_s\gamma$ observation.

It is useful to separately consider two different scenarios for $B \to X_s l^+ l^-$ decay which depend upon the sign of R_7:

Case 1. We accept all points in the MSSM parameter space for which $0.4 < R_7 < 1.2$. The extremal MSSM values we then find for our $B \to X_s l^+ l^-$ observables are displayed in Table II as fractions of their standard model counterparts. Looking at the entries in the table, we see that sensitivity of the nonresonant branching ratios to supersymmetry is fairly minimal. The reason for the slight variation can be traced to the coefficients of the R_Y and R_Z terms in Eqs. (5.10) and (5.11) which are considerably larger than those for the R_7 terms. Since R_Y and R_Z do not vary significantly from unity and the magnitude of R_7 is constrained by experiment, supersymmetric effects in the MSSM with a universal as well as more general soft sector are never highly pronounced in the nonresonant branching ratios.

On the other hand, the relatively larger coefficient of the R_7 term in Eq. (5.13) induces greater sensitivity in asymmetry observables to supersymmetric deviations from the standard model. In Fig. 3, we plot the ratio of the electron asymmetry observable $\mathcal{A}(B \to X_s e^+ e^-)_{NR}$ evaluated in the universal soft sector MSSM relative to its standard model value. This ratio is displayed in the figure as a function of $A_0(M_{GUT})$ and $m_0(M_{GUT})$ on a two-dimensional slice through the MSSM parameter space with $m_{\widetilde{w}}(m_z) = 150$ GeV, $\tan\beta = 20$, and $\text{sgn}(\mu) = +1$ held fixed. Looking at the Lego plot, we see a substantial volume in parameter space exists where supersymmetric deviations from the standard model are sizable.

Case 2. We accept all points in the MSSM parameter space for which $-4.2 < R_7 < -2.4$. Scans over the parameter space of the MSSM with GUT-scale universality then reveal that R_7 never dips below -2.5. This limiting value coincides with the lower end of the experimentally permissible $B \to X_s\gamma$ partial width range. It is important to note that $\Gamma(B \to X_s e^+ e^-)$ is strongly correlated with $\Gamma(B \to X_s\gamma)$ since a large short distance contribution to $B \to X_s e^+ e^-$ comes from the small dielectron mass region where the intermediate photon is only slightly off shell. Maximal suppression of the radiative rate therefore leads to a 10% suppression of the semielectronic rate. On the other hand, $\Gamma(B \to X_s\mu^+\mu^-)$ and $\Gamma(B \to X_s\gamma)$ are anticorrelated for $R_7 < 0$ due to the $C_7^{\text{eff}}\text{Re}[C_9^{\text{eff}}(\hat{s})]$ term in Eq. (5.2). The semimuonic branching fraction increases by 20% when $R_7 = -2.5$. More importantly, sizable signals of supersymmetry can be detected in the asymmetry observable. $\mathcal{A}_{NR}$ increases relative to its standard model value by factors of 3.6 and 2.6 for $B \to X_s e^+ e^-$ and $B \to X_s\mu^+\mu^-$ when $R_7 \simeq -2.5$.

If we again relax the universal soft sector assumptions, we find many points in the more general nine-dimensional parameter space where R_7 drops down to the lower end of its experimentally allowed range. The nonresonant $B \to X_s e^+ e^-$ and $B \to X_s\mu^+\mu^-$ branching ratios are then enhanced by up

to 90 and 110 %. Lepton asymmetries are also enhanced by approximately a factor of 3 compared to standard model expectations when R_7 belongs to the allowed negative range.[6]

The two different scenarios we have investigated for the impact of supersymmetry upon $B \to X_s l^+ l^-$ decay clearly have different phenomenological implications. The likelihood that this FCNC process will display interesting evidence for supersymmetry or else usefully constrain the MSSM parameter space strongly depends upon the value for R_7. After more precise experimental measurements and next-to-leading order theoretical calculations are completed in the near future, the allowed range for R_7 should shrink by about a factor of 3. It is possible that the standard model prediction $R_7 = 1$ will then no longer be consistent with CLEO data. Such a result would represent an intriguing finding.

At the present time, the CLEO measurement provides no means for determining the sign of the $b \to s\gamma$ amplitude. However, the current 3.5σ discrepancy between the standard model and data from the LERN $e^+ e^-$ collider LEP for $\Gamma(Z \to bb)$ may suggest that R_7 is negative in the MSSM framework. Large positive MSSM corrections to $\Gamma(Z \to b\bar{b})$ would ameliorate the conflict between theory and experiment. As such positive corrections are correlated with negative values for R_7, our second $B \to X_s l^+ l^-$ scenario may be favored. In this case, sizable deviations in $B \to X_s l^+ l^-$ branching ratios and lepton asymmetries from standard-model expectations should hopefully be detected in the next few years.

VI. CONCLUSIONS

In this work, we have studied the impact of supersymmetry upon the FCNC processes $K_L \to \pi^0 e^+ e^-$, $B \to X_s e^+ e^-$, and $B \to X_s\mu^+\mu^-$. We found that the rate for the kaon mode does not vary from standard model predictions by much more than 10% in the minimal supersymmetric extension with a universal soft breaking sector. Qualitatively similar results hold for the B meson nonresonant branching fraction. Since the premise underlying the MSSM with GUT-scale universality is not necessarily realized in nature, we have also considered these transitions in a more general class of models in which certain soft sector assumptions were relaxed. We then uncovered regions in a nine-dimensional parameter space where $B(B \to X_s l^+ l^-)_{NR}$ is significantly enhanced relative to its standard model value. Charge conjugation odd lepton asymmetries can exhibit even larger deviations from standard model expectations. So signals of supersymmetry could be detected in $B \to X_s l^+ l^-$ decay in the next few years.

Various refinements upon the analysis which we have presented in this paper could be pursued. For instance, radiative corrections to the MSSM scalar potential will alter the allowed regions of parameter space. Similarly, imposition of additional constraints arising from electroweak precision measurements and cosmological considerations would further restrict MSSM parameters. Although such refinements

---

[6]It is interesting to note that deviations of R_7 from unity in case 2 can induce larger variations in $\Gamma(B \to X_s l^+ l^-)_{MSSM}/\Gamma(B \to X_s l^+ l^-)_{SM}$ than in $\Gamma(B \to X_s\gamma)_{MSSM}/\Gamma(B \to X_s\gamma)_{SM}$.

TABLE II. Extremal MSSM values of $B \to X_s l^+ l^-$ observables as fractions of their standard model counterparts.

Observable	MSSM with universal soft sector		MSSM with relaxed soft sector assumptions	
	Minimal	Maximal	Minimal	Maximal
$B(B \to X_s e^+ e^-)_{\text{NR}}$	77%	107%	72%	119%
$\mathcal{A}(B \to X_s e^+ e^-)_{\text{NR}}$	80%	170%	81%	196%
$B(B \to X_s \mu^+ \mu^-)_{\text{NR}}$	88%	102%	71%	121%
$\mathcal{A}(B \to X_s \mu^+ \mu^-)_{\text{NR}}$	85%	148%	86%	164%

cannot affect our qualitative FCNC conclusions, they may somewhat alter our quantitative results.

More interestingly, the general approach which we have followed in this paper to investigate supersymmetric contributions to a particular class of rare modes can be applied to several other processes that might reveal larger discrepancies with the standard model. For example, our analysis of semileptonic $d_i \to d_j l^+ l^-$ decay can readily be extended to its neutrino analogue $d_i \to d_j \nu \bar{\nu}$. Similar methods can also be used to look for weak scale supersymmetry in $K \to \mu^+ \mu^-$, $B \to \tau^+ \tau^-$ and $B - \bar{B}$ mixing. Theoretical and experimental study of all these processes will help to constrain whatever physics lies beyond the standard model which is still waiting to be discovered.
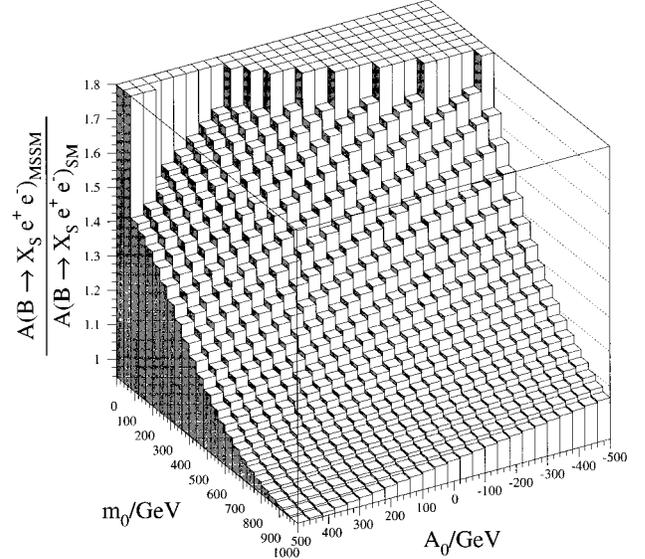
FIG. 3. Ratio of the nonresonant electron asymmetry observable $\mathcal{A}(B \to X_s e^+ e^-)_{\text{NR}}$ calculated in the MSSM relative to its standard-model value. The ratio is plotted as a function of $A_0(M_{\text{GUT}})$ and $m_0(M_{\text{GUT}})$ with $m_{\tilde{w}}(m_z) = 150$ GeV and $\tan \beta = 20$ held fixed. Excluded MSSM parameter space points are indicated in the plot by Lego blocks saturated at their maximum values.

APPENDIX A: MSSM $b \to s\gamma$ MATCHING CONDITIONS

We list below the W-scale matching contributions to the coefficient C_7 of the magnetic moment operator in the $\Delta B = 1$ effective Hamiltonian which arise from one-loop MSSM diagrams.

Standard-model graphs:

$$\delta C_7 = \frac{x_t}{4} f_1(x_t). \tag{A1}$$

Graphs with charged Higgs loops:

$$\delta C_7 = \frac{1}{6} \left\{ \frac{1}{2} \frac{m_t^2}{m_{h\pm}^2} \cot^2 \beta f_1 \left(\frac{m_t^2}{m_{h\pm}^2} \right) + f_2 \left(\frac{m_t^2}{m_{h\pm}^2} \right) \right\}. \tag{A2}$$

Graphs with chargino loops:

$$\delta C_7 = \frac{1}{3 g_2^2 K_{ts}^* K_{tb}} \sum_{A=1}^{6} \sum_{I=1}^{2} \frac{m_w^2}{m_{\tilde{\chi}_I^\pm}^2} \left\{ -\frac{1}{2} (X_I^{U_L})_{2A}^\dagger (X_I^{U_L})_{A3} f_1 \left(\frac{m_{\tilde{u}_A}^2}{m_{\tilde{\chi}_I^\pm}^2} \right) + (X_I^{U_L})_{2A}^\dagger (X_I^{U_R})_{A3} \frac{m_{\tilde{\chi}_I^\pm}}{m_b} f_2 \left(\frac{m_{\tilde{u}_A}^2}{m_{\tilde{\chi}_I^\pm}^2} \right) \right\}. \tag{A3}$$

Graphs with neutralino loops:

$$\delta C_7 = -\frac{1}{3 g_2^2 K_{ts}^* K_{tb}} \sum_{A=1}^{6} \sum_{I=1}^{4} \frac{m_w^2}{m_{\tilde{\chi}_I^0}^2} \left\{ \frac{1}{2} (Z_I^{D_L})_{2A}^\dagger (Z_I^{D_L})_{A3} f_3 \left(\frac{m_{\tilde{d}_A}^2}{m_{\tilde{\chi}_I^0}^2} \right) + (Z_I^{D_L})_{2A}^\dagger (Z_I^{D_R})_{A3} \frac{m_{\tilde{\chi}_I^0}}{m_b} f_4 \left(\frac{m_{\tilde{d}_A}^2}{m_{\tilde{\chi}_I^0}^2} \right) \right\}. \tag{A4}$$

Graphs with gluino loops:

$$\delta C_7 = \frac{4 g_3^2}{9 g_2^2 K_{ts}^* K_{tb}} \sum_{A=1}^{6} \frac{m_w^2}{m_{\tilde{g}}^2} \left\{ -(\Gamma^{D_L})_{2A}^\dagger (\Gamma^{D_L})_{A3} f_3 \left(\frac{m_{\tilde{d}_A}^2}{m_{\tilde{g}}^2} \right) + 2(\Gamma^{D_L})_{2A}^\dagger (\Gamma^{D_R})_{A3} \frac{m_{\tilde{g}}}{m_b} f_4 \left(\frac{m_{\tilde{d}_A}^2}{m_{\tilde{g}}^2} \right) \right\}. \tag{A5}$$

The one-loop integral functions that enter into these matching conditions are given by

$$f_1(x) = \frac{-7 + 5x + 8x^2}{6(1-x)^3} - \frac{2x - 3x^2}{(1-x)^4} \ln x,$$

$$f_2(x) = \frac{3x - 5x^2}{2(1-x)^2} + \frac{2x - 3x^2}{(1-x)^3} \ln x,$$

$$f_3(x) = \frac{2 + 5x - x^2}{6(1-x)^3} + \frac{x}{(1-x)^4} \ln x,$$

$$f_4(x) = \frac{1 + x}{2(1-x)^2} + \frac{x}{(1-x)^3} \ln x. \tag{A6}$$

APPENDIX B: MSSM $\bar{s} \to \bar{d} e^+ e^-$ AND $b \to s e^+ e^-$ MATCHING CONDITIONS

We tabulate below the W-scale matching contributions to the Y^{SUSY} and Z^{SUSY} parameters which appear in the Wilson coefficients y_{7V} and y_{7A} of the strange sector semileptonic operators Q_{7V} and Q_{7A} in Eq. (4.2). These same formulas hold for Wilson coefficients of analogous operators in the bottom sector. The KM matrix label q and numerical index i respectively equal $q = d$, $i = 1$ and $q = b$, $i = 3$ for $\bar{s} \to \bar{d} e^+ e^-$ and $b \to s e^+ e^-$ decay.

Z-penguin and bubble graphs with charged Higgs loops:

$$\delta Y^{\text{SUSY}} = \delta Z^{\text{SUSY}} = -\frac{1}{8} \cot^2\beta \, x_t f_5\left(\frac{m_t^2}{m_{h^\pm}^2}\right). \tag{B1}$$

γ-penguin and bubble graphs with charged Higgs loops:

$$\delta Y^{\text{SUSY}} = 0,$$

$$\delta Z^{\text{SUSY}} = -\frac{1}{72} \cot^2\beta \, f_6\left(\frac{m_t^2}{m_{h^\pm}^2}\right). \tag{B2}$$

Z-penguin and bubble graphs with chargino loops:

$$\delta Y^{\text{SUSY}} = \delta Z^{\text{SUSY}} = \frac{1}{2g_2^2 K_{ts}^* K_{tq}} \sum_{A,B=1}^{6} \sum_{I,J=1}^{2} (X_I^{U_L})_{2A}^\dagger (X_J^{U_L})_{Bi} \left\{ c_2(m_{\tilde{\chi}_I^\pm}^2, m_{\tilde{u}_A}^2, m_{\tilde{u}_B}^2)(\Gamma^{U_L}\Gamma^{U_L\dagger})_{AB}\delta_{IJ} \right.$$

$$\left. - c_2(m_{\tilde{u}_A}^2, m_{\tilde{\chi}_I^\pm}^2, m_{\tilde{\chi}_J^\pm}^2)\delta_{AB}V_{I1}^* V_{J1} + \frac{1}{2} m_{\tilde{\chi}_I^\pm} m_{\tilde{\chi}_J^\pm} c_0(m_{\tilde{u}_A}^2, m_{\tilde{\chi}_I^\pm}^2, m_{\tilde{\chi}_J^\pm}^2)\delta_{AB} U_{I1} U_{J1}^* \right\}. \tag{B3}$$

γ-penguin and bubble graphs with chargino loops:

$$\delta Y^{\text{SUSY}} = 0,$$

$$\delta Z^{\text{SUSY}} = \frac{1}{36g_2^2 K_{ts}^* K_{tq}} \sum_{A=1}^{6} \sum_{I=1}^{2} \frac{m_W^2}{m_{\tilde{u}_A}^2} (X_I^{U_L})_{2A}^\dagger (X_I^{U_L})_{Ai} f_7\left(\frac{m_{\tilde{\chi}_I^\pm}^2}{m_{\tilde{u}_A}^2}\right). \tag{B4}$$

Z-penguin and bubble graphs with neutralino loops:

$$\delta Y^{\text{SUSY}} = \delta Z^{\text{SUSY}} = \frac{1}{2g_2^2 K_{ts}^* K_{tq}} \sum_{A,B=1}^{6} \sum_{I,J=1}^{4} (Z_I^{D_L})_{2A}^\dagger (Z_J^{D_L})_{Bi} \left\{ c_2(m_{\tilde{\chi}_I^0}^2, m_{\tilde{d}_A}^2, m_{\tilde{d}_B}^2)(\Gamma^{D_R}\Gamma^{D_R\dagger})_{AB}\delta_{IJ} \right.$$

$$\left. - c_2(m_{\tilde{d}_A}^2, m_{\tilde{\chi}_I^0}^2, m_{\tilde{\chi}_J^0}^2)\delta_{AB}(N_{I3}^* N_{J3} - N_{I4}^* N_{J4}) - \frac{1}{2} m_{\tilde{\chi}_I^0} m_{\tilde{\chi}_J^0} c_0(m_{\tilde{d}_A}^2, m_{\tilde{\chi}_I^0}^2, m_{\tilde{\chi}_J^0}^2)\delta_{AB}(N_{I3} N_{J3}^* - N_{I4} N_{J4}^*) \right\} \tag{B5}$$

γ-penguin and bubble graphs with neutralino loops:

$$\delta Y^{\text{SUSY}} = 0,$$

$$\delta Z^{\text{SUSY}} = -\frac{1}{216g_2^2 K_{ts}^* K_{tq}} \sum_{A=1}^{6} \sum_{I=1}^{4} \frac{m_W^2}{m_{\tilde{d}_A}^2} (Z_I^{D_L})_{2A}^\dagger (Z_I^{D_L})_{Ai} f_8\left(\frac{m_{\tilde{\chi}_I^0}^2}{m_{\tilde{d}_A}^2}\right). \tag{B6}$$

Z-penguin and bubble graphs with gluino loops:

$$\delta Y^{\text{SUSY}} = \delta Z^{\text{SUSY}} = \frac{4g_3^2}{3g_2^2 K_{ts}^* K_{tq}} \sum_{A,B=1}^{6} (\Gamma^{D_L})_{2A}^\dagger (\Gamma^{D_L})_{Bi} c_2(m_{\tilde{g}}^2, m_{\tilde{d}_A}^2, m_{\tilde{d}_B}^2)(\Gamma^{D_R}\Gamma^{D_R\dagger})_{AB}. \tag{B7}$$

γ-penguin and bubble graphs with gluino loops:

$$\delta Y^{\text{SUSY}} = 0,$$

$$\delta Z^{\text{SUSY}} = -\frac{g_3^2}{81 g_2^2 K_{ts}^* K_{tq}} \sum_{A=1}^{6} \frac{m_W^2}{m_{\tilde{d}_A}^2} (\Gamma^{D_L})_{2A}^\dagger (\Gamma^{D_L})_{Ai} f_8\left(\frac{m_{\tilde{g}}^2}{m_{\tilde{d}_A}^2}\right). \tag{B8}$$

Chargino box graph:[7]

$$\delta Y^{\text{SUSY}} = \frac{m_W^2}{g_2^2 K_{ts}^* K_{tq}} \sum_{A=1}^{6} \sum_{I,J=1}^{2} (X_I^{U_L})_{2A}^\dagger (X_J^{U_L})_{Ai} d_2(m_{\tilde{\chi}_I^\pm}^2, m_{\tilde{\chi}_J^\pm}^2, m_{\tilde{u}_A}^2, m_{\tilde{\nu}_1}^2) V_{I1}^* V_{J1},$$

$$\delta Z^{\text{SUSY}} = 0. \tag{B9}$$

Neutralino box graphs:

$$\delta Y^{\text{SUSY}} = 2\sin^2\theta \, \delta Z^{\text{SUSY}} + \frac{m_W^2}{2 g_2^2 K_{ts}^* K_{tq}} \sum_{A=1}^{6} \sum_{I,J=1}^{4} (Z_I^{D_L})_{2A}^\dagger (Z_J^{D_L})_{Ai} \{ d_2(m_{\tilde{\chi}_I^0}^2, m_{\tilde{\chi}_J^0}^2, m_{\tilde{d}_A}^2, m_{\tilde{e}_1}^2)(N_{I2}^* + \tan\theta N_{I1}^*)(N_{J2} + \tan\theta N_{J1})$$

$$+ \tfrac{1}{2} m_{\tilde{\chi}_I^0} m_{\tilde{\chi}_J^0} d_0(m_{\tilde{\chi}_I^0}^2, m_{\tilde{\chi}_J^0}^2, m_{\tilde{d}_A}^2, m_{\tilde{e}_1}^2)(N_{I2} + \tan\theta N_{I1})(N_{J2}^* + \tan\theta N_{J1}^*)\},$$

$$\delta Z^{\text{SUSY}} = \frac{m_W^2}{g_2^2 K_{ts}^* K_{tq}} \sum_{A=1}^{6} \sum_{I,J=1}^{4} (Z_I^{D_L})_{2A}^\dagger (Z_J^{D_L})_{Ai} \sec^2\theta [d_2(m_{\tilde{\chi}_I^0}^2, m_{\tilde{\chi}_J^0}^2, m_{\tilde{d}_A}^2, m_{\tilde{e}_4}^2) N_{I1}^* N_{J1}$$

$$+ \tfrac{1}{2} m_{\tilde{\chi}_I^0} m_{\tilde{\chi}_J^0} d_0(m_{\tilde{\chi}_I^0}^2, m_{\tilde{\chi}_J^0}^2, m_{\tilde{d}_A}^2, m_{\tilde{e}_4}^2) N_{I1} N_{J1}^*]. \tag{B10}$$

The one-loop integral functions which appear within these MSSM matching conditions are given by

$$f_5(x) = \frac{x}{1-x} + \frac{x}{(1-x)^2} \ln x,$$

$$f_6(x) = \frac{38x - 79x^2 + 47x^3}{6(1-x)^3} + \frac{4x - 6x^2 + 3x^4}{(1-x)^4} \ln x,$$

$$f_7(x) = \frac{52 - 101x + 43x^2}{6(1-x)^3} + \frac{6 - 9x + 2x^3}{(1-x)^4} \ln x,$$

$$f_8(x) = \frac{2 - 7x + 11x^2}{(1-x)^3} + \frac{6x^3}{(1-x)^4} \ln x,$$

$$c_0(m_1^2, m_2^2, m_3^2) = -\left(\frac{m_1^2 \ln(m_1^2/\mu^2)}{(m_1^2 - m_2^2)(m_1^2 - m_3^2)} + (m_1 \leftrightarrow m_2) + (m_1 \leftrightarrow m_3) \right),$$

$$c_2(m_1^2, m_2^2, m_3^2) = \frac{3}{8} - \frac{1}{4}\left[\frac{m_1^4 \ln(m_1^2/\mu^2)}{(m_1^2 - m_2^2)(m_1^2 - m_3^2)} + (m_1 \leftrightarrow m_2) + (m_1 \leftrightarrow m_3) \right],$$

$$d_0(m_1^2, m_2^2, m_3^2, m_4^2) = -\left[\frac{m_1^2 \ln(m_1^2/\mu^2)}{(m_1^2 - m_2^2)(m_1^2 - m_3^2)(m_1^2 - m_4^2)} + (m_1 \leftrightarrow m_2) + (m_1 \leftrightarrow m_3) + (m_1 \leftrightarrow m_4) \right],$$

$$d_2(m_1^2, m_2^2, m_3^2, m_4^2) = -\frac{1}{4}\left[\frac{m_1^4 \ln(m_1^2/\mu^2)}{(m_1^2 - m_2^2)(m_1^2 - m_3^2)(m_1^2 - m_4^2)} + (m_1 \leftrightarrow m_2) + (m_1 \leftrightarrow m_3) + (m_1 \leftrightarrow m_4) \right]. \tag{B11}$$

All dependence upon the renormalization scale μ cancels out from the total supersymmetric matching conditions in Y^{SUSY} and Z^{SUSY}.

_____

[7]Our chargino and neutralino box graph matching condition results differ from those reported in [16] by overall signs.

[1] J. Ellis, G. L. Fogli, and E. Lisi, Phys. Lett. B **324**, 173 (1994); **333**, 118 (1994); P. H. Chankowski and S. Pokorski, *ibid.* **366**, 188 (1996); P. Langacker, NST Report No. NSF-ITP-95-140 hep-ph/9511207, 1995 (unpublished).

[2] B. de Carlos and J. A. Casas, Phys. Lett. B **349**, 300 (1995); V. Barger, M. S. Berger, P. Ochmann, and R. J. N. Philipps, Phys. Rev. D **51**, 2438 (1995); E. Gabrielli, A. Masiero, and L. Silverstrini, Report No. ROM2F/95/23, hep-ph/9510215, 1995 (unpublished); G. C. Cho, Y. Kizukuri, and N. Oshimo, Phys. Lett. B **372**, 101 (1996).

[3] CLEO Collaboration, M. S. Amal *et al.*, Phys. Rev. Lett. **74**, 2885 (1995).

[4] R. Barbieri and G. F. Giudice, Phys. Lett. B **309**, 86 (1993); R. Garisto and J. N. Ng, *ibid.* **315**, 372 (1993).

[5] Particle Data Group, L. Montanet *et al.*, Phys. Rev. D **50**, 1173 (1994).

[6] B. Winstein and L. Wolfenstein, Rev. Mod. Phys. **65**, 1113 (1993); K. Arisaka *et al.*, ''KAMI conceptual design report,'' Fermilab Report No. FN-568, 1991 (unpublished); Y. Wah (private communication).

[7] CLEO Collaboration, R. Balest *et al.*, in *Proceedings of the 27th International Conference on High Energy Physics*, Glasgow, Scotland, 1994, edited by P. J. Bussey and I. G. Knowles (IOP, London, 1995).

[8] CDF Collaboration, C. Anway-Wiese *et al.*, Fermilab Report No. Fermilab-Conf-95/201-E, 1995 (unpublished).

[9] J. M. Flynn and L. Randall, Nucl. Phys. **B326**, 31 (1989).

[10] C. O. Dib, I. Dunietz, and F. J. Gilman, Phys. Rev. D **39**, 2639 (1989).

[11] A. J. Buras, M. E. Lautenbacher, M. Misiak, and M. Munz, Nucl. Phys. **B423**, 349 (1994).

[12] M. Misiak, Nucl. Phys. **B393**, 23(E) (1993); **439**, 461 (1995); A. J. Buras and M. Münz, Phys. Rev. D **52**, 186 (1995).

[13] A. G. Cohen, G. Ecker, and A. Pich, Phys. Lett. B **304**, 347 (1993).

[14] G. Ecker, A. Pich, and E. de Rafael, Nucl. Phys. **B303**, 665 (1988); A. Pich, in *Introduction to Chiral Perturbation Theory*, Proceedings of the Fifth Mexican School of Particles and Fields, 1992, edited by J. L. Lucio M. and M. Vargas (American Institute of Physics, New York, 1994), p. 95.

[15] J. F. Donoghue and F. Gabbiani, Phys. Rev. D **51**, 2187 (1995).

[16] S. Bertolini, F. Borzumati, A. Masiero, and G. Ridolfi, Nucl. Phys. **B353**, 591 (1991).

[17] A. Ali, G. F. Giudice, and T. Mannel, Z. Phys. C **67**, 417 (1995).

[18] H. E. Haber and G. L. Kane, Phys. Rep. **117**, 75 (1985).

[19] H. E. Haber, in *Introductory Low-Energy Supersymmetry*, Proceedings of the Theoretical Advanced Study Institute, 1992, edited by J. Harvey and J. Polchinski (World Scientific, Singapore, 1993), p. 827.

[20] J.-P. Derendinger, in *Lecture Notes on Globally Supersymmetric Theories in Four and Two Dimensions*, Proceedings of the Hellenic School of Elementary Particle Physics, 1989, edited by E. N. Argyres, N. Tracas, and G. Zoupanos (World Scientific, Singapore, 1990), p. 790.

[21] L. Ibanez and G. Ross, Phys. Lett. **110B**, 215 (1982); L. Ibanez, Nucl. Phys. **B218**, 514 (1983).

[22] K. Inoue *et al.*, Prog. Theor. Phys. **68**, 927 (1982).

[23] L. Alvarez-Gaume, M. Claudson, and M. Wise, Nucl. Phys. **B207**, 96 (1982).

[24] J. Rosiek, Phys. Rev. D **41**, 3464 (1990).

[25] A. H. Chamseddine, R. Arnowitt, and P. Nath, Phys. Rev. Lett. **49**, 970 (1982); S. Soni and A. Weldon, Phys. Lett. **126B**, 215 (1983); L. Hall, J. Lykken, and S. Weinberg, Phys. Rev. D **27**, 2359 (1983); R. Barbieri, S. Ferrara, and C. A. Savoy, Phys. Lett. **119B**, 343 (1983); H. P. Nilles, M. Srednicki, and D. Wyler, *ibid.* **120B**, 346 (1983); R. Barbieri, J. Louis, and M. Moreti, *ibid.* **312**, 451 (1993).

[26] W. Buchmüller and D. Wyler, Phys. Lett. **121B**, 321 (1983); J. Polchinski and M. B. Wise, *ibid.* **125B**, 393 (1983).

[27] ALEPH Collaboration, L. Rolandi, OPAL Collaboration, H. Dijkstra, L3 Collaboration, D. Strickland, and OPAL Collaboration, G. Wilson (unpublished).

[28] J. Ellis, G. Ridolfi, and F. Zwirner, Phys. Lett. B **257**, 83 (1991).

[29] A. J. Buras, M. Misiak, M. Münz, and S. Pokorski, Nucl. Phys. **B424**, 374 (1994).

[30] B. Grinstein, M. J. Savage, and M. B. Wise, Nucl. Phys. **B319**, 271 (1989).

[31] A. F. Falk, M. Luke, and M. J. Savage, Phys. Rev. D **49**, 3367 (1994).

[32] S. Ferrara and E. Remiddi, Phys. Lett. **53B**, 347 (1974).

[33] Z. Ligeti and M. Wise, Phys. Rev. D **53**, 4937 (1996).